Density-driven instabilities in capillary tubes: Influence of a variable diffusion coefficient

S. H. Vanaparthy, C. Barthe,[a] and E. Meiburg
Department of Mechanical Engineering, University of California, Santa Barbara, California 93106-5070

(Received 16 December 2005; accepted 15 February 2006; published online 4 April 2006)

The influence of a variable diffusion coefficient on the gravitational instability at the interface between two variable viscosity fluids in a vertical capillary tube is investigated, based on the three-dimensional Stokes equations. As the viscosity contrast between the fluids grows, the maximum density gradient of the self-similar base concentration profile increases while its location is shifted into the more viscous fluid. Thus the perturbations are forced to grow in a more viscous environment, which can reduce their growth rate by up to 30%. For large viscosity contrasts, intermediate interface thicknesses are seen to give rise to the highest growth rates. For most parameter combinations, the first azimuthal mode is found to be most unstable. However, for large viscosity ratios and small interface thicknesses the axisymmetric mode dominates.
© *2006 American Institute of Physics*. [DOI: 10.1063/1.2192447]

The gravitational instability at the interface separating a heavier fluid above from a lighter fluid below represents a classical problem in fluid mechanics (Batchelor and Nitsche[1]). Vanaparthy *et al.*[2] analyzed the miscible version of this instability in a vertical capillary tube, based on the three-dimensional Stokes equations, in order to study how its growth is affected by the presence of sidewalls. A comprehensive review of the pertinent literature is provided by those authors. Subsequently, Payr *et al.*[3] extended this investigation to fluids of different viscosities. They report that the growth rates do not depend on whether the heavier or the lighter fluid is the more viscous one, and that in the presence of large viscosity contrasts thicker interfaces may be more unstable than thinner ones. The first azimuthal mode is generally found to be most unstable, in agreement with the experimental observations of Kuang *et al.*[4] and the three-dimensional nonlinear simulations of Wilhelm and Meiburg.[5] However, for large viscosity contrasts and thin interfaces, the axisymmetric mode may have a larger growth rate than its azimuthal counterpart. Corresponding findings for Hele-Shaw configurations are reported by Graf *et al.*[6] and Goyal and Meiburg.[7]

All of the above investigations employed a constant diffusion coefficient. Especially for fluids with widely disparate viscosities, this is known to be a poor approximation of the real situation. For example, the measurements by Petitjeans and Maxworthy[8] clearly show that for water and glycerin the diffusion coefficient varies strongly with the concentration (cf. also the experiments of Rashidnia and Balasubramaniam[9] and the simulations of Chen and Meiburg[10] and Riaz *et al.*[11]). Hence, a detailed analysis of the influence of a variable diffusion coefficient is the goal of the present investigation. For this purpose, we utilize the well-established Stokes–Einstein relation (Probstein[12]), according to which the diffusion coefficient is inversely proportional to the fluid viscosity. While this relation does not hold for all fluid mixtures, cf. Zwanzig and Harrison,[13] it is well suited as basis for a first exploration of the effects of a variable diffusion coefficient.

We consider an unstable, miscible interface that separates a lighter fluid from a heavier one placed above it, in a vertically oriented capillary tube of diameter d. The two fluids of different viscosities are assumed to be miscible with each other in all proportions, with a diffusion coefficient $D(c)$ that depends on the concentration c. Since the flow velocities are small, the fluid motion is governed by the three-dimensional Stokes equations. The density $\rho=\rho_2+c(\rho_1-\rho_2)$ and viscosity $\mu=\mu_2 e^{Rc}$ are assumed to be linear and exponential functions of the concentration, respectively. Here ρ_1 and μ_1 indicate the density and viscosity of the heavier fluid, while ρ_2 and μ_2 represent their counterparts for the lighter fluid. R denotes the logarithm of the viscosity contrast, $R=\ln(\mu_1/\mu_2)$. We assume the variation of the diffusion coefficient with concentration is governed by the generalized Stokes–Einstein relation (cf. Probstein[12]) $D(c)\cdot\mu(c)=\text{const.}$, so that $D=D_2 e^{-Rc}$, where D_2 denotes the diffusion coefficient of an infinitesimally small amount of the heavier fluid 1 in pure fluid 2.

The governing equations are rendered dimensionless by introducing a characteristic length $L^*=d$, viscosity $\mu^*=\mu_{\min}$, velocity $U^*=\Delta\rho g d^2/\mu_{\min}$, time $T^*=\mu_{\min}/\Delta\rho g d$, pressure $P^*=\Delta\rho g d$, and density difference $R^*=\Delta\rho=\rho_1-\rho_2$. The diffusion coefficient is referred to its average value $D^*=\int_0^1 D dc$, so that a meaningful comparison can be made with calculations assuming a constant diffusion coefficient. This implies that with an increasing value of R the diffusion coefficient varies over a larger range, while its average value remains unchanged.

By using the above relations in the Stokes equations, we obtain the set of dimensionless equations

$$\nabla\cdot\mathbf{u}=0, \tag{1}$$

[a]Present address: Ecole Polytechnique, 91128 Palaiseau, France.

 © 2006 American Institute of Physics

Downloaded 01 May 2006 to 128.111.70.242. Redistribution subject to AIP license or copyright, see http://pof.aip.org/pof/copyright.jsp

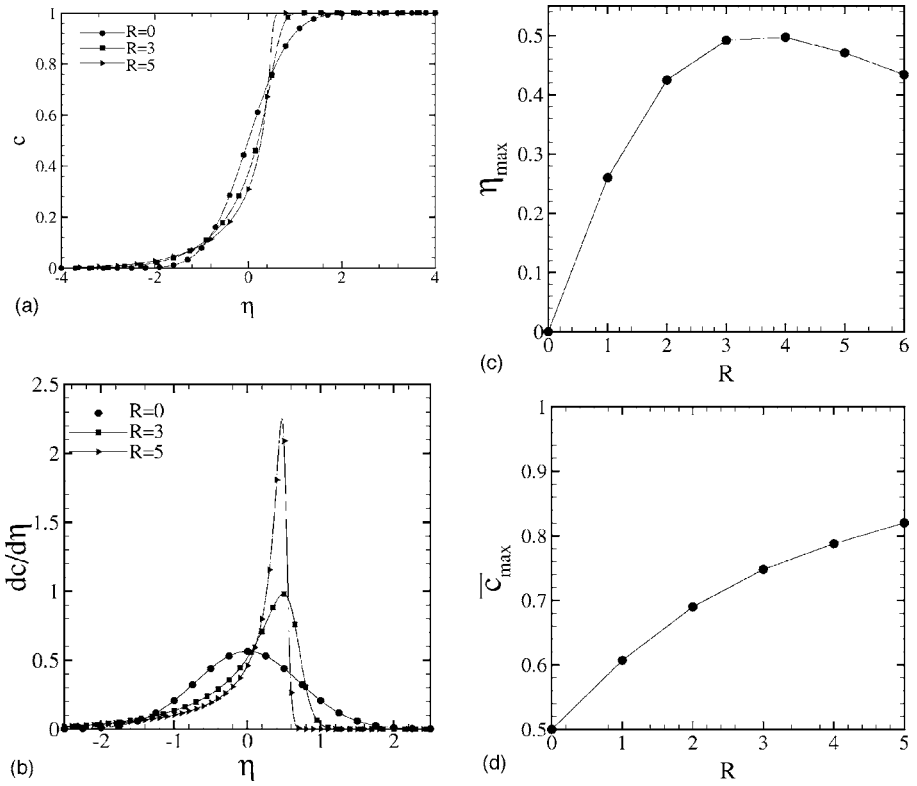

FIG. 1. Base profile properties as a function of the viscosity ratio R: (a) base profile; (b) gradient of the base profile; (c) location of the maximum gradient; (d) base concentration at this location.

$$\nabla p = \nabla \cdot \boldsymbol{\tau} - c\,\nabla z, \tag{2}$$

$$\frac{\partial c}{\partial t} + \mathbf{u}\cdot\nabla c = \frac{1}{Ra}\nabla\cdot(D\,\nabla c). \tag{3}$$

Here, the Rayleigh number $Ra = \Delta\rho g d^3/D^*\mu_{\min}$ provides a relative measure of the destabilizing buoyancy forces and the stabilizing effects of diffusion and viscosity. In treating these and related equations numerically, we adopt the approach outlined by Vanaparthy *et al.*[2] for the region near the axis.

For both of the fluids at rest everywhere, the base concentration profile $\bar{c}$ is a solution of the equation $\partial\bar{c}/\partial t = \partial/\partial z\left(D\,\partial\bar{c}/\partial z\right)$. By introducing the similarity variable $\eta = z/\sqrt{4D^*t}$, we obtain the nonlinear ordinary differential equation

$$-2\eta\frac{d\bar{c}}{d\eta} = e^{-R\bar{c}}\frac{R}{1-e^{-R}}\left[\frac{d^2\bar{c}}{d\eta^2} - R\left(\frac{d\bar{c}}{d\eta}\right)^2\right], \tag{4}$$

with the boundary conditions $\bar{c}(\eta\to\infty)=1$ and $\bar{c}(\eta\to-\infty)=0$. This equation is solved iteratively for $\bar{c}(\eta)$ in the control volume $-10\leqslant\eta\leqslant 10$, using second-order finite differences, until a converged profile is obtained. Test calculations showed this volume to be sufficiently large so that the boundaries have a negligible effect on the solution. As an initial condition for the iteration procedure we employ a linearly varying profile in the computational domain. Since the diffusive fluxes do not vanish exactly at the boundaries, mass conservation needs to be enforced by satisfying the additional integral condition $\int_{-\infty}^{\infty} c\,d\eta = \text{const}$.

Figure 1(a) shows the resulting base concentration profile as a function of the viscosity ratio R. For $R=0$, $\bar{c}$ is the symmetric error function profile. With increasing R, $\bar{c}$ becomes steeper in the more viscous fluid due to the locally weaker diffusion, and shallower in the less viscous fluid as a result of locally stronger diffusion. The shape of the profiles resembles the experimentally measured curves of Petitjeans and Maxworthy.[8] We remark that it remains meaningful to refer to $z=0$ as the interface location, as there are equal amounts of fluid 2 above, and fluid 1 below the interface, respectively. The gradient of the base concentration profile is plotted as function of the viscosity ratio in Fig. 1(b). The maximum slope of the concentration profile is seen to grow with R. The resulting increase in the local Rayleigh number Ra_l, formed with the local density gradient rather than the overall density difference, is expected to be destabilizing. From (4) we obtain the location of the maximum gradient, i.e., the location of the inflection point, as

$$\eta_{\max} = e^{-R\bar{c}}\frac{R^2}{2(1-e^{-R})}\left(\frac{d\bar{c}}{d\eta}\right)_{\max}. \tag{5}$$

Since all of the terms on the right-hand side of this equation are positive, $\eta_{\max}$ is positive for all values of R. This is confirmed by Fig. 1(c), which quantifies the upward shift of the location of the maximum slope. This shift reaches a maximum for a value of R between 3 and 4, and subsequently decreases for larger R values. Figure 1(d) shows that the concentration, and hence the viscosity, at this location of the maximum slope increases monotonically with R. This should have a stabilizing effect, as the perturbation will grow more slowly in a more viscous environment.

We now consider small perturbations to this base state of the form $\hat{c}(r,z)\cos(\beta\theta)e^{\sigma t}$, where the hatted quantity represents the two-dimensional eigenfunction, and β denotes the azimuthal wave number. For the purpose of evaluating the

Downloaded 01 May 2006 to 128.111.70.242. Redistribution subject to AIP license or copyright, see http://pof.aip.org/pof/copyright.jsp

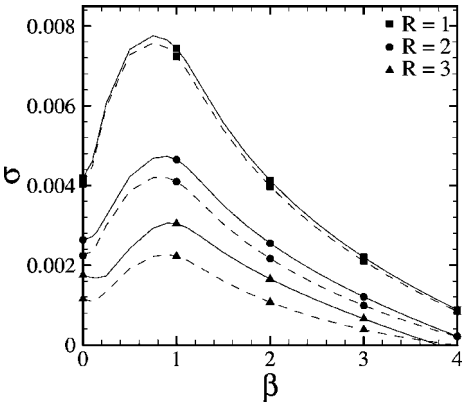

FIG. 2. Growth rate σ as a function of the azimuthal wave number β for D=const. (—) and $D=D(c)$ (- -), with $Ra=10^5$, $\delta=0.5$, and various R. The variable diffusion coefficient consistently results in a reduced growth rate.

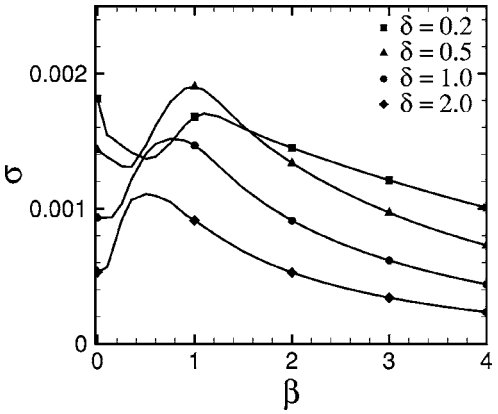

FIG. 3. Dispersion relations for various values of δ, $Ra=10^7$ and $R=4$. For these parameters, intermediate interface thicknesses can exhibit the highest growth rates.

stability of these perturbations, we assume that the diffusive time scale of the base state is much larger than the characteristic time scale of the instability growth, so that the base state can be held constant. Note that, since the linear stability analysis is conducted in the original (not similarity) variables, the interface thickness denoted by δ represents an independent parameter. By substituting the above relations into the dimensionless governing equations, subtracting out the base state and linearizing, we obtain an eigenvalue problem of the form $\mathbf{A}\phi=\sigma\mathbf{B}\phi$, where σ is the growth rate and $\phi=(\hat{\mathbf{u}},\hat{p},\hat{c})$ denotes the eigenvector. This system is solved for σ and ϕ as functions of the azimuthal wave number β, for various combinations of Ra, R, and δ, as discussed by Vanaparthy *et al.*[2]

An inspection of the concentration eigenfunction contours for the cases $R=2$ (more viscous fluid on top) and $R=-2$ (more viscous fluid at the bottom) shows that they represent mirror images of each other, as their maxima are shifted in opposite directions, i.e., always toward the more viscous fluid. The growth rates are identical. A simple transformation shows that, if a solution to the linearized perturbation equations is given by σ, R_+, $\bar{c}_{R+}(z)$, $\hat{c}_{R+}(r,z)$, and $\hat{u}_{z,R+}(r,z)$, another solution to the same equation with the same value of σ is of the form

$$R_- = -R_+, \tag{6}$$

$$\bar{c}_{R-}(z) = 1 - \bar{c}_{R+}(-z), \tag{7}$$

$$\hat{c}_{R-}(r,z) = \hat{c}_{R+}(r,-z), \tag{8}$$

$$\hat{u}_{z,R-}(r,z) = \hat{u}_{z,R+}(r,-z). \tag{9}$$

For this reason, we will limit our discussion to positive values of the viscosity ratio only, in which the upper heavier fluid is the more viscous one.

We carried out corresponding calculations with both constant (*CD*) and variable (*VD*) diffusion coefficients, respectively. Figure 2(a) displays the leading eigenvalue as a function of the azimuthal wave number β for the representative case of $Ra=10^5$, $\delta=0.5$, and various R. It should be noted that even though only integral values of β are physically meaningful, the dispersion relations are drawn as continuous curves in order to guide the eye. As expected, an increase in R has a stabilizing influence, while larger values of Ra are seen to result in higher growth rates. Moreover, the results show that for all (Ra,R) combinations, the *VD* growth rates are consistently lower than their *CD* counterparts, by up to 30% for larger values of R. This result is remarkable, considering that the average diffusion coefficient for *VD* is equal to the constant diffusion coefficient for *CD*, so that the overall damping influence of diffusion should be comparable for the two cases.

Dispersion relations for various values of R and δ show that the growth rates generally increase with Ra until they reach an asymptotic plateau for $Ra>10^7$. For moderate values of R and δ, the azimuthal mode $\beta=1$ is more unstable than its axisymmetric counterpart. However, Fig. 3 demonstrates that for a thinner interface with $\delta=0.2$, a higher viscosity ratio $R=4$, and large Ra the axisymmetric mode can exhibit a higher growth rate than the azimuthal one. Moreover, for $R=4$ the highest growth rate occurs for an intermediate value of the interfacial thickness. With *CD* a similar observation had been made by Payr *et al.*[3] These authors attribute this behavior to the shift of the eigenfunctions into the less viscous fluid or the region of least damping influence. Visual inspection of the eigenfunctions for *VD* shows that this shift into the less viscous fluid persists at high Ra and R, thus allowing the growth rates for thicker interfaces to be higher than those for thinner ones.

The above observations raise the question as to what determines the location of the eigenfunction maximum, along with its growth. For a given value of the interface thickness δ, the two governing dimensionless parameters are R and Ra, respectively. It is important to realize that they enter the problem in different ways. The viscosity ratio R, and with it the variability of the diffusion coefficient, determines both the base state and also enters directly into the perturbation equations for the concentration and the three components of momentum. Ra, on the other hand, does not affect the base concentration profile, and enters directly only into the equation for the concentration perturbation. The large Ra asymptotic regime presents us with an opportunity to analyze the influence of R in isolation. Towards this

Downloaded 01 May 2006 to 128.111.70.242. Redistribution subject to AIP license or copyright, see http://pof.aip.org/pof/copyright.jsp

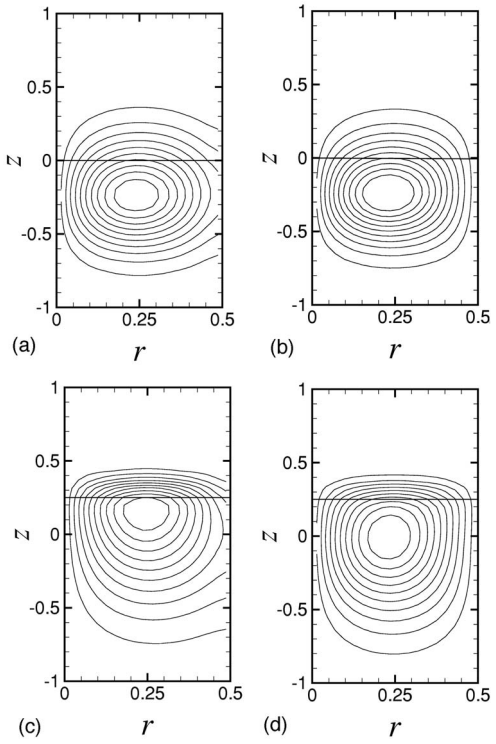

FIG. 4. Contours of $\hat{c}$ for *CD* (upper row) and *VD* (lower row) with $R=3$, $\delta=0.5$ and $\beta=1$. Left column: $Ra=10^5$, right column: $Ra=10^7$. The horizontal line indicates the location of the highest value of Ra_l.

end, we carried out four different sets of calculations for $Ra=10^7$. The largest growth rates are obtained for *CD*, i.e., a constant diffusion coefficient. Indistinguishable from these results are those obtained when the variable diffusion coefficient is accounted for only in the perturbation equation, but not in the base profile (*VDE*). This suggests that at large values of *Ra* the effect of the variable diffusion coefficient in the perturbation equations is negligible, so that its influence is felt only through the modification of the base profile. This observation is confirmed by the fact that the growth rates computed for a variable diffusion coefficient throughout (*VD*) are identical to those obtained when the diffusion coefficient is kept constant in the perturbation equations (*VDB*), as long as the variable diffusion base profile is accounted for.

For a lower value of $Ra=10^5$, the situation is different. The highest growth rate is again observed for *CD*, but the results for *VDE* are now significantly lower. This indicates that at lower *Ra* the variability of the diffusion coefficient in the perturbation equations is important. In agreement with this, the results for *VDB* are still noticeably higher than those for *VD*, confirming that the base profile effect cannot account for all of the difference between *CD* and *VD*.

An important quantity with regard to the instability growth is the *local* Rayleigh number Ra_l, formed with the local density gradient $d\rho/dc$ rather than the global density difference $\Delta\rho$. As a result of invoking the Stokes–Einstein assumption, the denominator of Ra_l is constant throughout the flow field, so that Ra_l depends on the local density gradient only. As we saw above, this density gradient reaches its maximum at a location $z_{\max}(R)>0$, which causes the upward shift of the eigenfunction maximum as R increases. The competition of Ra_l and the local viscosity with regard to determining the location of the eigenfunction maximum are summarized in Fig. 4. For $D=$const., shown in the upper row, the steepest slope and the highest local Rayleigh number occur at $z=0$. The viscosity profile causes the eigenfunction maximum to be shifted downward from the location of the steepest slope, i.e., into the less viscous fluid, where the perturbation can grow faster. The shift is nearly identical for the Rayleigh number of 10^5 and 10^7. For $D=D(c)$, on the other hand, shown in the lower row, the steepest slope and the highest value of Ra_l occur at a location $z>0$. Again the eigenfunction maximum is shifted downwards from this location due to the viscosity profile. This shift is more pronounced for the higher Rayleigh number of 10^7. Here the local value Ra_l is in the asymptotic regime over a much larger section of the interfacial region. Within this section, the growth rate becomes independent of Ra_l, and thus mostly is a function of the local viscosity. Hence for $Ra=10^7$ the eigenfunction maximum is able to move into a less viscous environment as compared to the lower value of $Ra=10^5$.

In summary, in the asymptotic large Rayleigh number regime the modification of the base concentration profile dominates, while for lower Rayleigh numbers the effects of the concentration-dependent diffusion coefficient are also felt through the perturbation equations.

Support for this research was received from the NASA Microgravity and NSF/ITR programs, and through an NSF equipment grant.

[1] G. K. Batchelor and J. M. Nitsche, "Instability of stratified fluid in a vertical cylinder," J. Fluid Mech. **252**, 419 (1993).
[2] S. H. Vanaparthy, E. Meiburg, and D. Wilhelm, "Density-driven instabilities of miscible fluids in a capillary tube: linear stability analysis," J. Fluid Mech. **497**, 99 (2003).
[3] M. Payr, S. H. Vanaparthy, and E. Meiburg, "Influence of variable viscosity on density-driven instabilities of miscible in capillary tubes," J. Fluid Mech. **525**, 333 (2005).
[4] J. Kuang, T. Maxworthy, and P. Petitjeans, "Velocity fields and streamline patterns of miscible displacements in cylindrical tubes," Exp. Fluids **22**, 271 (2003).
[5] D. Wilhelm and E. Meiburg, "Three-dimensional spectral element simulations of variable density and viscosity, miscible displacements in a capillary tube," Comput. Fluids **33**, 485 (2004).
[6] F. Graf, E. Meiburg, and C. Härtel, "Density-driven instabilities of miscible fluids in a Hele-Shaw cell: Linear stability analysis of the three-dimensional Stokes equations," J. Fluid Mech. **451**, 261 (2002).
[7] N. Goyal and E. Meiburg, "Unstable density stratification of miscible fluids in a vertical Hele-Shaw cell: Influence of variable viscosity on the linear stability analysis," J. Fluid Mech. **516**, 211 (2004).
[8] P. Petitjeans and T. Maxworthy, "Miscible displacements in capillary tubes. Part 1. Experiments," J. Fluid Mech. **326**, 37 (1996).
[9] N. Rashidnia and R. Balasubramaniam, "Measurement of the mass diffusivity of miscible liquids as a function of concentration using a common path shearing interferometer," Exp. Fluids **36**, 619 (2004).
[10] C. Y. Chen and E. Meiburg, "Miscible displacements in capillary tubes. Part 2. Numerical simulations," J. Fluid Mech. **326**, 57 (1996).
[11] A. Riaz, C. Pankiewitz, and E. Meiburg, "Linear stability of radial displacements in porous media: Influence of velocity-induced dispersion and concentration-dependent diffusion," Phys. Fluids **16**, 3592 (2004).
[12] R. F. Probstein, *Physicochemical Hydrodynamics* (Wiley, New York, 1994).
[13] R. Zwanzig and A. K. Harrison, "Modifications of the Stokes-Einstein formula," J. Chem. Phys. **83**, 5861 (1985).

Downloaded 01 May 2006 to 128.111.70.242. Redistribution subject to AIP license or copyright, see http://pof.aip.org/pof/copyright.jsp